ORIGINAL ARTICLE

Treatment of pancreatic fibrosis with siRNA against a collagen-specific chaperone in vitamin A-coupled liposomes

Hirotoshi Ishiwatari,[1] Yasushi Sato,[1] Kazuyuki Murase,[1] Akihiro Yoneda,[2] Ryosuke Fujita,[2] Hiroki Nishita,[2] Naoko Kubo Birukawa,[2] Tsuyoshi Hayashi,[1] Tsutomu Sato,[1] Koji Miyanishi,[1] Rishu Takimoto,[1] Masayoshi Kobune,[1] Shigenori Ota,[3] Yasutoshi Kimura,[3] Koichi Hirata,[3] Junji Kato,[1] Yoshiro Niitsu[2]

▶ Additional supplementary files are published online only. To view these files please visit the journal online (http://dx.doi.org/10.1136/gutjnl-2011-301746).

[1]Fourth Department of Internal Medicine, Sapporo Medical University, Sapporo, Japan
[2]Department of Molecular Target Exploration, Sapporo Medical University,Sapporo, Japan
[3]First Department of Surgery, Sapporo Medical University, Sapporo, Japan

Correspondence to
Professor Yoshiro Niitsu, Department of Molecular Target Exploration, Sapporo Medical University School of Medicine, South 1, West 17, Chuo-ku, Sapporo 060-8543, Japan; niitsu@sapmed.ac.jp

HI, YS and KM contributed equally to this work.

Received 27 September 2012
Accepted 12 October 2012
Published Online First
20 November 2012

▶ http://dx.doi.org/10.1136/gutjnl-2012-303937

To cite: Ishiwatari H, Sato Y, Murase K, *et al*. *Gut* 2013;**62**:1328–1339.

ABSTRACT

Background and objective Fibrosis associated with chronic pancreatitis is an irreversible lesion that can disrupt pancreatic exocrine and endocrine function. Currently, there are no approved treatments for this disease. We previously showed that siRNA against collagen-specific chaperone protein gp46, encapsulated in vitamin A-coupled liposomes (VA-lip-siRNAgp46), resolved fibrosis in a model of liver cirrhosis. This treatment was investigated for pancreatic fibrosis induced by dibutyltin dichloride (DBTC) and cerulein in rats.

Methods Specific uptake of VA-lip-siRNAgp46, conjugated with 6′-carboxyfluorescein (FAM) by activated pancreatic stellate cells (aPSCs), was analysed by fluorescence activated cell sorting (FACS). Intracellular distribution of VA-lip-siRNAgp46-FAM was examined by fluorescent microscopy. Suppression of gp46 expression by VA-lip-siRNAgp46 was assessed by immunoblotting. Collagen synthesis in aPSCs was assayed by dye-binding. Specific delivery of VA-lip-siRNAgp46 to aPSCs in DBTC rats was verified following intravenous VA-lip-siRNA-FAM and ^{3}H-VA-lip-siRNAgp46. The effect of VA-lip-siRNA on pancreatic histology in DBTC- and cerulein-treated rats was determined by Azan-Mallory staining and hydroxyproline content.

Results FACS analysis revealed specific uptake of VA-lip-siRNAgp46-FAM through the retinol binding protein receptor by aPSCs in vitro. Immunoblotting and collagen assay verified knockdown of gp46 and suppression of collagen secretion, respectively, by aPSCs after transduction of VA-lip-siRNAgp46. Specific delivery of VA-lip-siRNAgp46 to aPSCs in fibrotic areas in DBTC rats was confirmed by fluorescence and radioactivity 24 h after the final injection. 10 systemic VA-lip-siRNAgp46 treatments resolved pancreatic fibrosis, and suppressed tissue hydroxyproline levels in DBTC- and cerulein-treated rats.

Conclusion These data suggest the therapeutic potential of the present approach for reversing pancreatic fibrosis.

Significance of this study

What is already known on this subject?
- Pancreatic fibrosis is an irreversible lesion that can disrupt pancreatic function; there are no approved treatments.
- The accumulation of fibrotic tissue results from sustained activation of pancreatic stellate cells (PSCs).
- The characteristics of PSCs resemble those of hepatic stellate cells (HSCs).
- We have previously succeeded in resolving liver fibrosis in cirrhotic rat models by targeting HSCs with vitamin A coupled liposomes which carried siRNA against the collagen specific chaperone protein gp46.

What are the new findings?
- Rat activated PSCs take up vitamin A-coupled liposomes (VA-lip-siRNAgp46) in a retinol binding protein-mediated fashion, similarly to activated HSCs.
- Transduction of siRNAgp46 in activated PSCs caused suppression of collagen secretion.
- Activated PSCs specifically took up siRNAgp46 encapsulated in vitamin A liposomes in the pancreas of dibutyltin dichloride (DBTC)-treated rats.
- VA-lip-siRNAgp46 treatments resolved pancreatic fibrosis, and suppressed tissue hydroxyproline levels in DBTC- and cerulein-treated rats.
- This is the first demonstration of successful targeting of antifibrotic drug to both cells and molecule which are responsible for pancreatic fibrosis.

How might it impact on clinical practice in the foreseeable future?
- Results suggest the therapeutic potential of the present approach for reversing pancreatic fibrosis.

INTRODUCTION

Chronic pancreatitis is characterised by inflammation and replacement of parenchymal cells with fibrotic tissue leading to functional alterations, such as debilitating exocrine and occasional endocrine insufficiency. The accumulation of fibrotic tissue results from sustained activation of pancreatic stellate cells (PSCs), which proliferate and secrete collagen in response to stimulation by cytokines, growth factors, and reactive oxygen species from inflammatory cells

and damaged pancreatic tissue.[1 2] Various approaches to suppress the activation of PSCs and to eradicate activated PSCs (aPSCs) have been explored for the prevention and treatment of fibrosis associated with chronic pancreatitis.[3–5] However, so far no clinically applicable agents have been developed, mainly because of the inability for specific drug delivery to aPSCs.

We previously demonstrated complete resolution of liver cirrhosis in rat models using vitamin A-coupled liposomes to specifically deliver siRNA against the collagen-specific chaperone, gp46 (VA-lip-siRNAgp46), to hepatic stellate cells (HSCs) via the circulating receptor for retinol binding protein (RBP).[6] The characteristics of PSCs, including collagen synthesis, storage of vitamin A, expression of gp46, etc, resemble those of HSCs.[7] Therefore, in the present study, we examined whether our previous therapeutic approach for liver cirrhosis could be successfully applied for the treatment of pancreatic fibrosis.

MATERIALS AND METHODS

Preparation of siRNAgp46 and its conjugate with 6′-carboxyfluorescein

A formulation of siRNA directed against gp46, a rat homologue of human HSP47, was purchased from Hokkaido System Science (Sapporo, Japan). The sense and anti-sense strands of siRNAs have been described in detail previously.[6] For fluorescence activated cell sorting (FACS) analyses and in vivo tracing of gp46siRNA, gp46 siRNA with 6′-carboxyfluorescein (6-FAM) -coupled to the 5′ end of the sense strand was used.

A formulation of siRNA directed against HSP47 (GenBank accession no. 50454) was purchased from Hokkaido System Science. The sense and anti-sense strands of siRNAs were: HSP47, 5′-ggacaggccucuacaacuaTT-3′ (sense); 5′-uaguuguagaggccugucc TT-3′ (antisense).

Preparation of vitamin A-coupled liposomes carrying siRNAgp46

Vitamin A-coupled liposomes carrying siRNAgp46 (VA-lip-siRNAgp46) were prepared as described previously.[6]

Animals

Male Lewis rats (Charles River, Tokyo, Japan), weighing 150–200 g, and male Wistar rats (Charles River), weighing 250–300 g, were used for dibutyltin dichloride (DBTC) and cerulein experiments, respectively. All animal procedures were approved by the Sapporo Medical College Institutional Animal Care and Use Committee.

Isolation and cultivation of rat PSCs

Rat PSCs were isolated by density gradient centrifugation, as detailed previously.[8] All experiments were performed with culture-activated cells (aPSCs, passage 1–3).

Isolation and cultivation of human PSCs

Human pancreases were obtained during surgery for chronic pancreatitis. All these patients were seen at Sapporo Medical University. Informed consent in writing was obtained from each patient. Human PSCs were isolated by outgrowth, using explant techniques from the pancreas as described previously.[1] In this study, experiments were performed on activated α-smooth muscle actin (SMA)-positive cells between the first and third serial passages using lines.

FACS analysis of VA-lip-siRNAgp46-FAM

Rat aPSCs were cultivated with VA-lip-siRNAgp46-FAM (50 nM of siRNA) for 30 min. For the blocking assay, 1×10^4 cells were treated with mouse anti-RBP antibody (10 μg/ml, BD Pharmingen, San Diego, California, USA) for 30 min before adding VA-lip-siRNAgp46-FAM. The mean fluorescence intensity of VA-lip-siRNAgp46-FAM-treated cells was assessed on a FACScalibur with CellQuest software (Becton Dickinson, San Jose, California, USA).

Intracellular distribution analysis of VA-lip-siRNAgp46-FAM

Distribution of VA-lip-siRNAgp46-FAM in aPSCs after transduction was analysed as described previously.[6]

Western blot analysis

Protein extracts of cells and pancreas specimens were resolved over 4/20 sodium dodecylsulphate–polyacrylamide gels, transferred onto nitrocellulose membranes, probed with antibodies against HSP47 (gp46) (Stressgen Biotechnologies, Victoria, BC, Canada) or β-actin (Cell Signaling, Beverly, Massachusetts, USA), and then probed with peroxidase-coupled antibodies as the secondary antibody (Oncogene Research Product, Boston, Massachusetts, USA). Lastly, the cells were visualised with ECL (Amersham Life Science, Arlington Heights, Illinois, USA). Western blots were quantified using ImageJ 1.43u (NIH, Bethesda, Maryland, USA).

Quantification of collagen production

Collagen production by rat aPSCs was measured according to the method described previously for aHSCs, except for cell cultivation period after transduction; 24 h for aHSCs and 72 h for aPSCs.[6 9]

Quantitative RT–PCR

Total RNA was isolated using RNeasy mini kits (Qiagen, Hilden, Germany). Total RNA (1 μg) was used for reverse transcription with SuperScript II (Invitrogen, Carlsbad, California, USA) plus RNaseOUT (Invitrogen) using random primers (Invitrogen) according to the manufacturer's instructions. All TaqMan primers mixed with probes (GAPDH, Rn 99999916_s1; MMP2, Rn 02532334_s1; COL1A1, Rn00801649_g1; TIMP-1, Rn 00587558_m1; Gp46, Rn 00367777_m1; TGFβ, Rn01475963_m1) were purchased from Applied Biosystems (Foster City, California, USA). The TaqMan reactions were performed using 7300 Fast Real Time PCR System (Applied Biosystems). The results were expressed as the ratio of the number of copies of the product gene to the number of copies of the housekeeping gene (GAPDH) from the same RNA (respective cDNA) sample and PCR run.

Induction of pancreatic and hepatic fibrosis by DBTC

Among several models of pancreatic fibrosis,[10–18] we chose the DBTC model in which the common bile duct is obstructed by a plug formed with necrotic biliopancreatic ductal epithelium, because the procedure is relatively simple to perform as compared with other models and irreversible pancreatitis can be induced by a single injection of DBTC. DBTC (Sigma, St Louis, Missouri, USA) was first dissolved in ethanol (1 part) and then mixed with glycerol (2 parts) and dimethyl sulfoxide (2 parts).[10] For administration of DBTC, we selected the right jugular vein route to avoid any possible damage of the tail vein caused by the tail vein route for subsequent application of VA-lip-siRNAgp46.[10] In preliminary experiments, we found the lethality rates of dosages 8.0, 7.0 and 5.0 mg/kg body weight to be 4/4 (100%), 7/16 (44%) and 5/27 (19%), respectively. Thus, we selected the dosage of 5.0 mg/kg for the main experiments (see online supplementary figure S1).

Fibrosis, as revealed by Azan-Mallory staining, was evident in pancreatic and hepatic specimens on days 29 and 43 of DBTC injection (see online supplementary figure S1A–C).

Induction of pancreatic fibrosis by cerulein

Male Wistar rats received two intraperitoneal injections of 50 μg/kg cerulein (Sigma) 1 h apart every week for 6 weeks, as described by Ishibashi (see online supplementary figure S2A,B).[18]

Collagenase activity in pancreas homogenates

Collagenase activity (collagen type I) in pancreas homogenates was measured as described previously.[19]

In vivo localisation of VA-lip-siRNArandom-FAM in rat pancreas

From day 43 of DBTC administration, rats were injected intravenously with 1 μl/g body weight of VA-lip-siRNArandom-FAM or Lip-siRNArandom-FAM (0.75 mg/kg siRNA) three times on alternating days. At 24 h after the last injection, the rats were sacrificed by saline perfusion. Pancreatic tissue was immediately embedded in OCT compound (Sakura Finetechnical, Tokyo, Japan) medium and cryogenically sectioned. Multicoloured fluorescent staining of sections and their analysis were carried out as described previously.[6]

Tissue distribution of radiolabelled VA-lip-siRNArandom

^{3}H-VA-lip-siRNArandom (200 μCi), prepared as described previously, was administered via the tail vein under normal pressure in either DBTC-treated rats (day 43) or normal rats. After 24 h, the rats were sacrificed under anaesthesia, and radioactivity of each tissue was assayed as described previously.[6]

Treatment of DBTC rats and cerulein rats with VA-lip-siRNAgp46 and measurement of hydroxyproline content

Three groups of rats (n=10 per group) were used for histological evaluations. From day 43 of DBTC or cerulein administration, Lip-siRNAgp46, VA-lip-siRNAgp46 (0.75 mg/kg siRNA) or phosphate buffered saline (PBS; three times a week every other day) were injected for a total of 10 times via the tail vein under normal pressure in a volume of 1 μl/g body weight.[6] Hydroxyproline content in the pancreas was measured as previously described.[20]

Immunohistochemical staining for α-SMA

Pancreas was fixed with 10% paraformaldehyde. Then, immunohistochemical staining for α-SMA was performed by the dextran polymer method using monoclonal anti α-SMA antibody (1 : 1000, Sigma) and an Envision Kit (Dako), followed by colouring with 3, 3'-diaminobenzidine (DAB) and nuclear staining with Gill's haematoxylin solution. To accurately quantitate areas stained with α-SMA, slides from six randomly selected low-power fields (×100) per pancreas section from each rat were viewed by microscopy (Axioplan 2; Carl Zeiss) and the percentage of areas stained with α-SMA was quantified as previously described.[6]

In vitro apoptosis assay

Rat and human aPSCs under going apoptosis were stained with an in situ Cell Death Detection kit (Roche) according to the manufacturer's protocol. Slides were washed with PBS, and exposed to Prolong Gold Antifade Reagent with 4′, 6--diamidino-2-phenylindole (DAPI) (Molecular Probes) to stain nuclei. The number of terminal deoxynucleotidyl transferase-mediated deoxyuridine triphosphate nick-end labelling (TUNEL)-positive cells (green) in aPSCs were counted in 10 random high-power fields (×800) using fluorescent microscopy (Keyence, BZ-8000) for each sample.

Double staining of pancreas specimen for TUNEL and α-SMA

Double staining for TUNEL and α-SMA was undertaken and the number of TUNEL-positive apoptotic cells within the fibrotic bands was determined using a method modified from that described by Iredale *et al*.[19] Briefly, the specimen was first stained with an in situ Cell Death Detection kit (Roche) according to the manufacturer's protocol, followed by immunostaining for α-SMA (Sigma), with an alkaline phosphatase-conjugated anti-mouse second antibody (KPL, Gaithersburg, Maryland, USA) using a Vector Red alkaline phosphatase substrate kit 1 (Vector Lab, Peterborough, UK). The number of TUNEL-positive cells (brown) in α-SMA-positive areas (red), but not those in parenchymal area, were counted in 10 random high-power fields (×800).

Ethics approval

This research follows the tenets and regulations of the Declaration of Helsinki and has been approved by the Animal Care and the Institutional Review Board at Sapporo Medical University.

Statistics

Results are presented as mean±SD for each sample. Multiple comparisons between control groups and other groups were performed by Dunnet's test.

RESULTS

Specific uptake of RBP bound VA-lip-siRNAgp46 by rat aPSCs

Rat aPSCs, which were stained positive for α-SMA (figure 1A), were incubated with VA-lip-siRNAgp46-FAM or Lip-siRNAgp46-FAM in the presence of 10% fetal calf serum, and were observed under a fluorescence microscope. In VA-lip-siRNAgp46-FAM treated aPSCs, fluorescence appeared as a fine granular pattern in the cytoplasm at 30 min and as denser granular patterns in the perinuclear region at 2 h (figure 1B). In contrast, in Lip-siRNAgp46-FAM treated aPSCs, no green fluorescence was seen at 30 min and perinuclear fluorescence at 2 h was very faint (figure 1B). The fluorescence intensity of VA-lip-siRNAgp46-FAM aPSCs as revealed by FACS was clearly suppressed by RBP antibody to nearly the same level as Lip-siRNAgp46-FAM aPSCs (figure 1C).

Suppression of gp46 expression and collagen secretion of rat aPSCs by VA-lip-siRNAgp46

Treatment of aPSCs with VA-lip-siRNAgp46 brought about dose-dependent suppression of gp46 with almost complete suppression at 50 nM, which lasted at least 72 h (figure 1D,E) while treatment with VA-lip-siRNA random or Lip-siRNAgp46 did not cause any suppression. In the culture plate of VA-lip-siRNAgp46-treated aPSCs, significantly less collagen than that of VA-lip-siRNA random-treated or non-treated aPSCs was found (figure 1F).

Delivery of VA-lip-siRNArandom-FAM to aPSCs in vivo

The specific delivery of VA-lip-siRNArandom-FAM to aPSCs in the fibrotic pancreas was examined by fluorescent emission 24 h after three injections (figure 2A). Specimens were prepared from head (figure 2B,D) and body portions (figure 2C,E) of the pancreas. In both portions, fluorescence of

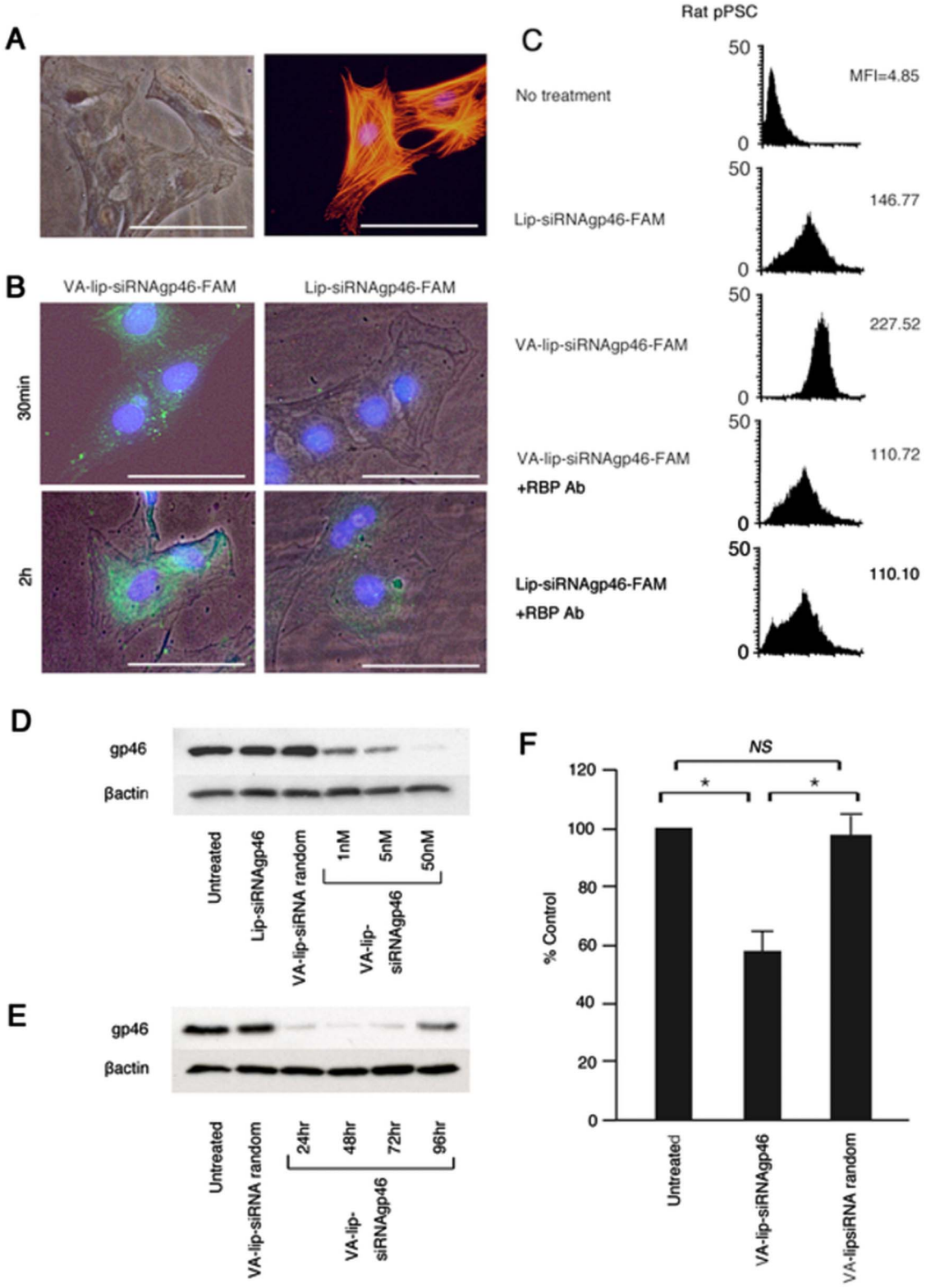

Figure 1 Retinol binding protein receptor-dependent uptake of vitamin A-coupled liposomes (VA-lip-siRNAgp46)-carboxyfluorescein (FAM) by activated pancreatic stellate cells (aPSCs) and suppressive effect of siRNAgp46 on gp46 expression and collagen synthesis. (A) Representative fluorescent images of rat aPSCs. Phase-contrast micrograph image of aPSCs (left panel) and immunofluorescent staining of aPSCs with Cy3-conjugated anti-α-SMA antibody (red) and nuclei counterstained with DAPI (blue) (right panel). Bars=100 μm. (B) Representative fluorescent images of the intracellular distribution of FAM-labelled siRNA. Rat aPSCs were treated with VA-lip-siRNAgp46-FAM or Lip-siRNAgp46-FAM. At 30 min, the medium was replaced with fresh medium. At the time indicated, cells were fixed and analysed by fluorescence microscopy to determine the relative intracellular distribution of siRNA-FAM (green). Bars=100 μm. One of five representative images is shown. (C) Representative fluorescence activated cell sorting patterns of rat PSCs treated with vitamin A-free liposomes carrying siRNAgp46-FAM (Lip-siRNAgp46-FAM) or VA-lip-siRNAgp46-FAM with or without anti-RBP antibody. Mean fluorescence intensity is indicated. Five independent experiments were carried out in each set of aPSCs and the results were essentially the same. (D) Western blotting was used to analyse the expression of gp46 and β-actin

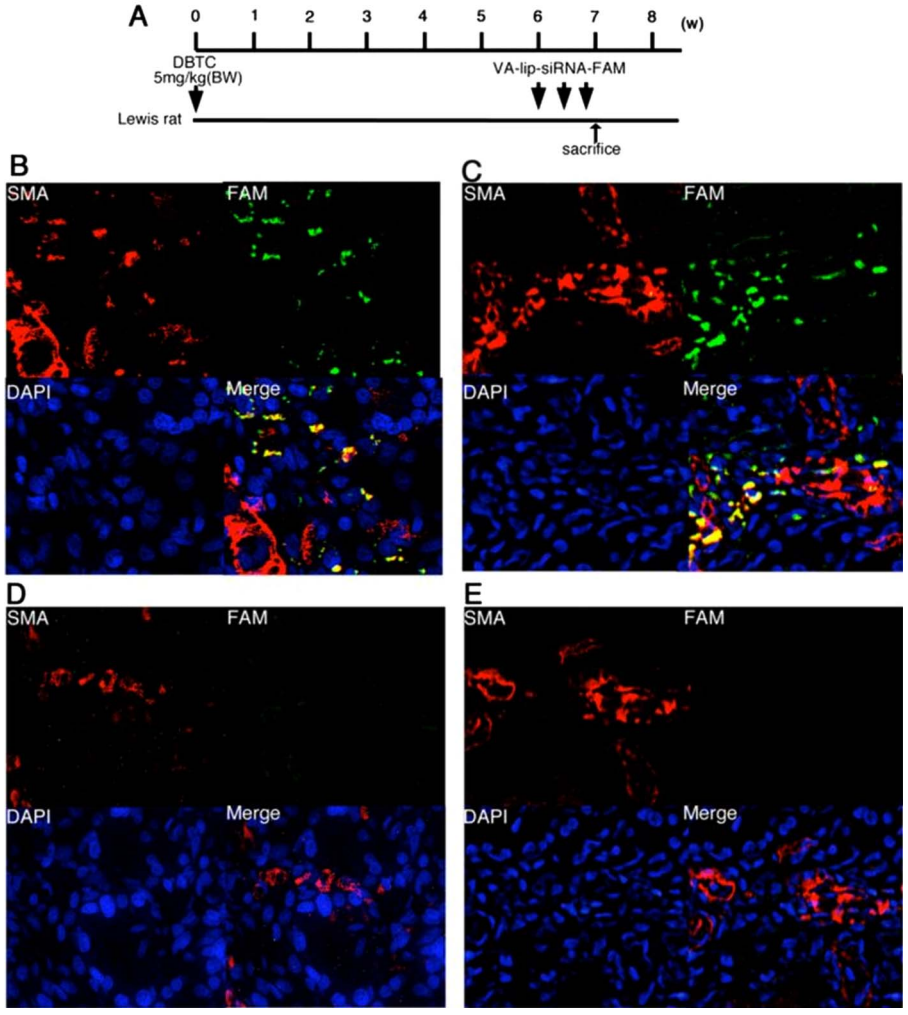

Figure 2 Specific delivery of vitamin A-coupled liposomes(VA-lip-siRNA) random-carboxyfluorescein (FAM) to activated pancreatic stellate cells (aPSCs) in dibutyltin dichloride (DBTC)-treated rats. (A) Schedule of VA-lip-siRNArandom-FAM injection in rats with DBTC-induced pancreatic fibrosis. Samples (B, D; pancreas head, C, E; pancreas body) were obtained from DBTC-treated rats that received three injections of VA-lip-siRNArandom-FAM or Lip-siRNArandom-FAM (siRNA doses of 0.75 mg/kg, 3 times every other day) (n=6 per group). Representative fluorescent images of α-SMA visualised by Cy3-conjugated anti-α-SMA antibody (red), nuclei counterstained with DAPI (blue) and siRNA random-FAM (green) in pancreas specimens obtained 24 h after the last injection. Pictures were taken at original magnification (×200). Fluorescence of siRNA random-FAM (green) was identified in pancreas, predominantly in the region that stained positive for α-SMA giving rise to areas with a merged yellow colour.

VA-lip-siRNArandom-FAM (green) was identified predominantly in the spotty region that stained positive only for α-SMA (aPSCs) (red), giving rise to a merged yellow colour (figure 2B,C). By contrast, in rats treated with Lip-siRNArandom-FAM, the yellow area in α-SMA positive regions was negligible (figure 2D,E).

The yellow area in six randomly selected high-power (×200) fields from each specimen occupied 32.1±10.5% of the area stained for α-SMA. By contrast, the yellow area in α-SMA-positive regions was negligible (2.0±1.5%) in a rat injected with lip-siRNAgp46-FAM.

To further elucidate the organ distribution, ^{3}H-labelled VA-lip-siRNArandom was administered to DBTC-treated rats with pancreatitis (day 43) and normal rats (table 1). Radioactivity in the pancreas of DBTC-treated rats was significantly higher (by approximately fivefold) than that of normal rats. In the liver, radioactivity in the DBTC group was also higher (approximately fourfold) than that of normal rats. Other organs, including the lungs, spleen and intestines, showed no increase in radioactivity in DBTC-treated rats, relative to normal rats.

Duration of gp46 suppression in aPSCs in the pancreas of DBTC rats treated with VA-lip-siRNAgp46

To examine the duration of effect of siRNAgp46 on gp46 expression, DBTC rats (n=15) were injected intravenously with VA-lip-siRNAgp46 on day 43 (see online supplementary figure S3A). The expression of gp46 in the pancreas of rats sacrificed at day 43, 44, 45, 46 and 47 (n=3 per group), was analysed by western blotting. The results for each rat per group were essentially the same. Representative western blot bands from one of three rats at each time-point and densitometric values are shown in online supplementary figure S3B,C. Suppression of gp46 expression started 24 h after initiated of treatment and lasted for at least 3 days.

Resolution of pancreatic fibrosis by VA-lip-siRNAgp46 in DBTC-treated rats

After 10 treatments with VA-lip-siRNAgp46 (figure 3A), an apparent reduction and statistically significant reduction analysed by computerised imaging of fibrosis represented by

(normalisation control) in aPSCs transfected with Lip-siRNAgp46,VA-lip-siRNA random or VA-lip-siRNAgp46. Dose-dependent inhibition of gp46 expression by siRNAgp46 was observed. (E) Duration of suppressive effect of siRNAgp46 on gp46 expression in aPSCs. Rat aPSCs were treated with VA-lip-siRNAgp46 or VA-lip-siRNA random. At 30 min, the medium was replaced with fresh medium. At the time indicated, the expression of gp46 and β-actin (normalisation control) was analysed by western blotting. Similar results were obtained in three independent experiments. (F) Collagen deposition on tissue culture plates was assayed by the dye-binding method 72 h after transduction in rat aPSCs treated with VA-lip-siRNAgp46 or with VA-lip-siRNArandom. Data are expressed as mean±SD calculated from five transductions and as a percentage of untreated control. *p<0.05 vs VA-lip-siRNAgp46. NS, not significant.

Table 1 Tissue biodistribution of (^{3}H)VA-lip-siRNAgp46 in rats

	Radioactivity (cpm/tissue)			
	Normal (×10^5)	DBTC rat (×10^5)	p Value (normal vs DBTC rat)	Ratio (DBTC rat/ normal)
Pancreas	0.481±0.270	2.42±0.840	0.001	5.03
Liver	77.2±21.0	319±105	0.002	4.14
Lung	3.83±1.89	5.26±3.66	NS	1.37
Spleen	1.75±0.740	1.84±1.11	NS	1.05
Intestine	4.23±1.59	4.52±1.00	NS	1.07

DBTC-treated rats (day 43 rat) and normal rats (n=3 per group) received a single intravenous injection of 200 μCi (^{3}H)VA-lip-siRNAgp46 via the tail vein. Tissue biodistribution was analysed 24 h later. Data represent means±SD (n=3). Similar results were obtained in two independent experiments.
DBTC, dibutyltin dichloride; NS, not significant; VA-lip-siRNAgp46, vitamin A-coupled liposomes.

Azan-Mallory positive area was confirmed (figure 3B,C). Results were consistent with data showing substantial suppression of hydroxyproline levels (figure 3D).

Disappearance of aPSCs following treatment with VA-lip-siRNAgp46

To elucidate of disappearance of aPSCs after treatment, immunostaining for α-SMA was performed. A substantially smaller area was stained for α-SMA in rats treated with VA-lip-siRNAgp46 compared to the stained area in rats treated with Lip-siRNAgp46 or PBS (figure 3E,F).

Effect of VA-lip-siRNAgp46 treatment on pancreatic inflammation in DBTC-treated rats

Since it is known that PSCs play a role not only in fibrosis but also in the inflammatory response,[21] we explored the effect of VA-lip-siRNAgp46 treatment on inflammation of pancreas in DBTC-treated rats. The degree of inflammation, assessed by cell infiltration, fatty change, tubular complex formation and infiltration of macrophages and T cells were reduced after treatment with VA-lip-siRNAgp46 (see online supplementary figure S4 and table S1).

Resolution of hepatic fibrosis by VA-lip-siRNAgp46 in DBTC-treated rats

In the DBTC model, hepatic fibrosis occurs in addition to pancreatic fibrosis because DBTC causes obstruction of the common bile duct (see online supplementary figure S5A,B). The Azan-Mallory positive area was significantly reduced in specimens from VA-lip-siRNAgp46-treated rats as compared with that in control specimens (see online supplementary figure S5C).

Apoptosis of siRNAgp46-induced aPSCs

We examined the possibility that apoptotic death of rat aPSCs may be induced by siRNAgp46 treatment in vitro. The number of TUNEL positive cells was greater in siRNAgp46-transfected aPSCs than in control aPSCs (figure 4A). The ratio of apoptotic nuclei to total nuclei of siRNAgp46-transfected aPSCs was 38.3±8.2% and was significantly increased relative to controls (figure 4B).

Apoptosis of aPSCs by siRNAHSP47 was also examined in human PSCs obtained by outgrowth from fibrotic human pancreas. TUNEL staining in apoptotic nuclei of siRNAHSP47-transfected aPSCs was higher than in control aPSCs (figure 4C). The ratio of apoptotic nuclei to total nuclei of siRNAHSP47-transfected aPSCs was 18.3±4.2% and was significantly increased relative to controls (figure 4D).

Furthermore, apoptosis of aPSCs by siRNAgp46 was examined in DBTC-treated rats. In DBTC pancreas, TUNEL positive cells in areas overlapping with aPSCs (α-SMA positive) also increased after treatment with VA-lip-siRNAgp46 (figure 4E,F).

Resolution of pancreatic fibrosis by VA-lip-siRNAgp46 in cerulein-treated rats

In the cerulein induced pancreatitis model (see online supplementary figure S2 and figure 5A), the therapeutic effect of VA-lip-siRNAgp46 was also evident with respect to shrinkage of the fibrotic area (figure 5B) and suppression of hydroxyproline levels (figure 5C).

Changes in mRNA expression of fibrosis-related proteins before and after administration of VA-lip-siRNAgp46 in DBTC-treated rats

We measured mRNA levels of gp46, collagen I, MMP2, TIMP-1, and TGFβ in pancreas homogenates from normal rats and DBTC-treated rats (figure 6A). The mRNA ratios relative to GAPDH mRNA are shown in figure 6B. mRNAs of gp46, collagen I, MMP2 and TGFβ expressed in aPSCs were increased in fibrotic pancreas as compared to normal pancreas. TIMP-1 mRNA levels did not increase but instead showed a slight decrease in response to induction of fibrosis. However, after treatment with VA-lip-siRNAgp46, the expression of all mRNAs was significantly decreased, presumably due to the disappearance of aPSCs.

Elevated collagenase activity in the pancreasof DBTC-treated rats

To confirm that sufficient collagenase activity to resolve the predeposited collagen resides in fibrotic pancreas, we measured collagenase activity in the pancreas homogenates of DBTC-treated rats after three injections of VA-lip-siRNAgp46 (day 49), and found that it was significantly higher than that of control normal rat and became even higher after treatment with VA-lip-siRNA gp46 (figure 6C).

Changes in microvessel density in fibrotic pancreas tissue before and after treatment with VA-lip-siRNAgp46

In DBTC-treated pancreas before VA-lip-siRNAgp46 treatment, the mean microvessel counts were 39±9.5. After 10 injections of VA-lip-siRNAgp46, the mean microvessel counts significantly reduced to 19±9.2 (see online supplementary figure S6).

DISCUSSION

PSCs have been shown to store vitamin A and synthesise collagen, and they can be activated by inflammatory cytokines, exerting functions similar to those of HSCs.[1 2 7] However, it has not been elucidated whether RBP is involved in vitamin A uptake. It is also not clear whether HSP47 is involved in collagen secretion by aPSCs. Therefore we first clarified that aPSCs indeed take up vitamin A in an RBP-mediated fashion by demonstrating that with VA-lip-siRNAgp46-FAM, but not with Lip-siRNAgp46-FAM, the fluorescence that appeared within 30 min of incubation was suppressed by anti-RBP antibody, and the amount of collagen on the culture plate of VA-lip-siRNAgp46-treated cells was significantly reduced (figure 1C,F). These findings verified the similarity of aPSCs to activated hepatic stellate cells in terms of RBP-mediated vitamin A uptake and gp46 -assisted collagen secretion.

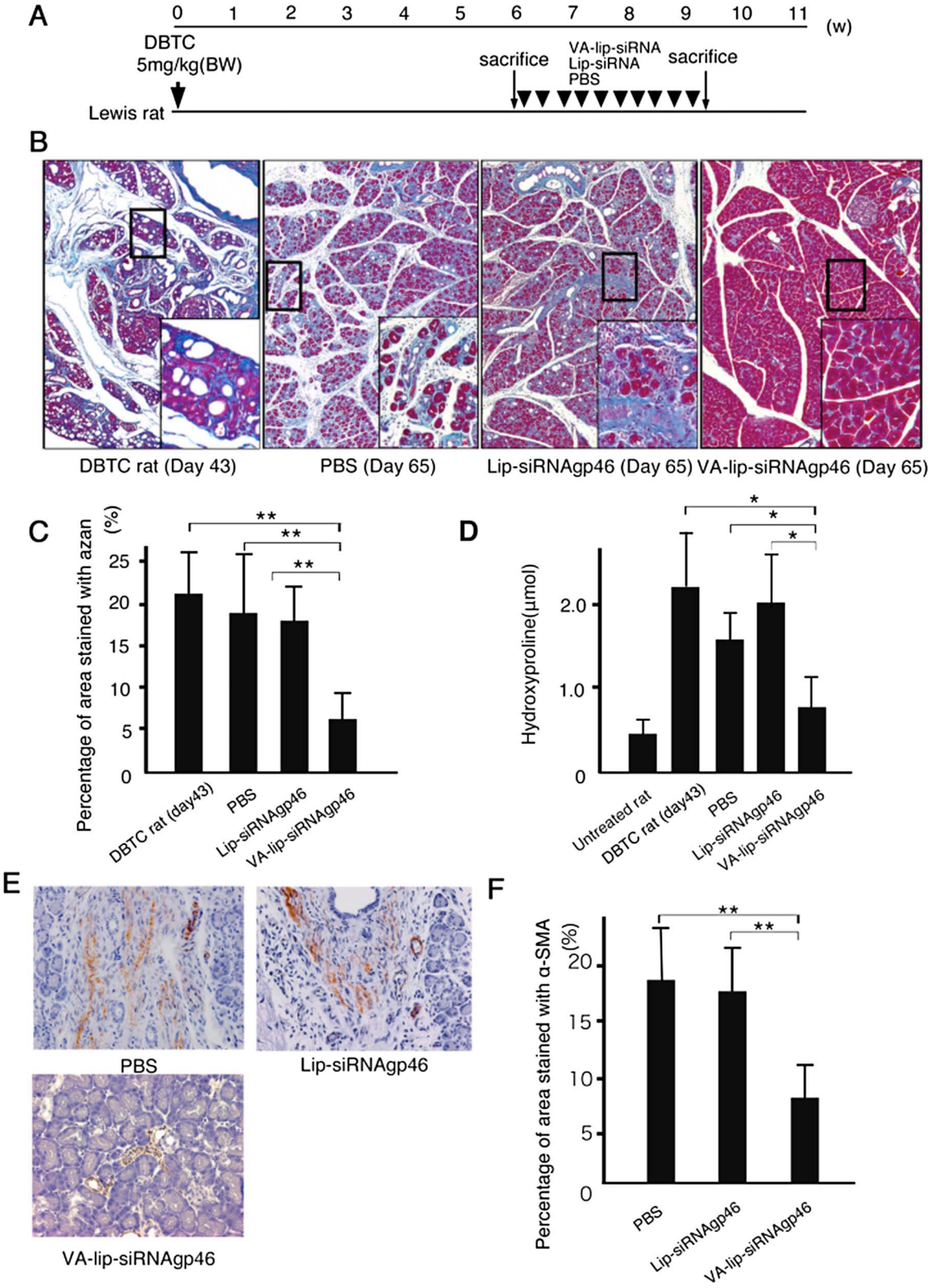

Figure 3 Effect of intravenous injected vitamin A-coupled liposomes (VA-lip-siRNAgp46) on dibutyltin dichloride (DBTC)-induced pancreatic fibrosis. (A) Schedule of VA-lip-siRNAgp46 treatment in rats with DBTC-induced pancreatic fibrosis. Samples were obtained from DBTC-treated rats that received 10 injections of VA-lip-siRNAgp46, Lip-siRNA gp46 (siRNA doses of 0.75 mg/kg, 3 times every other day), or PBS alone (n=10 per group). (B) Representative photomicrographs of Azan-Mallory stained pancreas section. Pictures were taken at original magnification (×100). Magnified images corresponding to the areas enclosed in boxes are presented as indicated. (C) Azan-Mallory positive staining area assessed by computerised image analysis. Data were obtained from six randomly selected fields in each of 10 rats from four groups and represent the mean±SD. (D) Hydroxyproline content in the pancreas. Mean±SD of 10 rats per group. (E) Representative immunohistochemical staining images of activated pancreatic stellate cells stained with anti-α-SMA antibody (brown). Pictures were taken at original magnification (×200). Results from each group of 10 rats were essentially similar. (F) α-SMA-positive staining area assessed by computerised image analysis. Data were obtained from six randomly selected fields in each of 10 rats from three groups and represent the mean±SD. *p<0.05; **p<0.01 vs VA-lip-siRNAgp46 treated- DBTC rat.

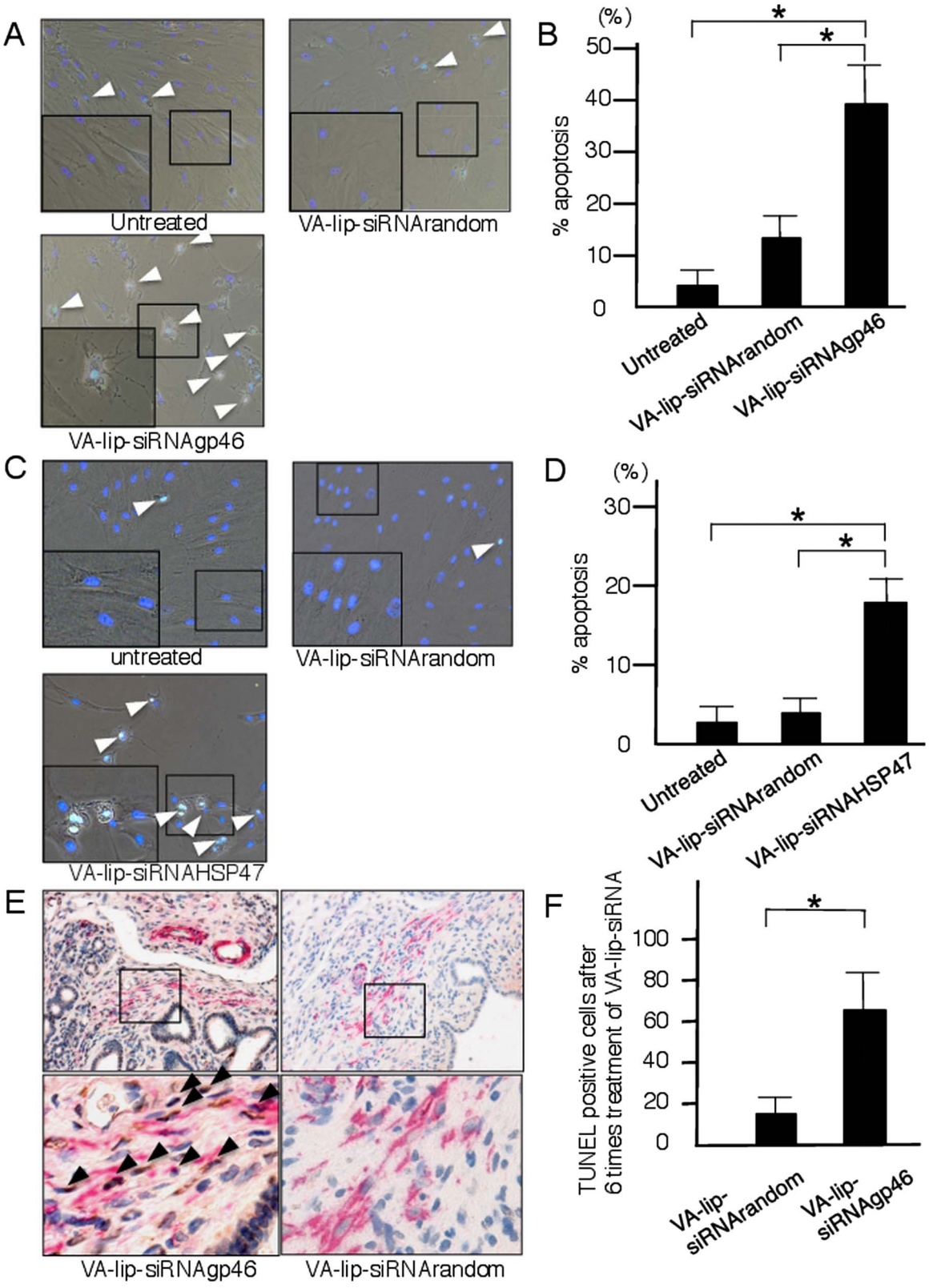

Figure 4 Apoptosis of activated pancreatic stellate cells (aPSCs) induced by vitamin A-coupled liposomes (VA-lip-siRNA) treatment. (A) Representative photomicrographs of rat aPSCs undergoing apoptosis. Nuclei of aPSCs treated with VA-lip-siRNAgp46 or with control agents were stained with FITC-transferase-mediated deoxyuridine triphosphate nick-end labelling (TUNEL) (green) and DAPI (blue) 72 h after each treatment. Arrowheads indicate apoptotic cells. Pictures taken at original magnification (×200) and magnified images corresponding to the areas enclosed in boxes are presented in the inset. (B) Quantification of apoptotic aPSCs shown in figure 4A. Apoptotic nuclei (green) and total nuclei (green + blue) were examined by fluorescent microscopy and counted in 10 randomly selected fields per slide for each indicated treatment; the ratios of apoptotic to normal nuclei were expressed as percentages. Results represent the mean±SD of three independent experiments. *p<0.01 vs VA-lip-siRNAgp46. (C) Representative photomicrographs of human aPSCs undergoing apoptosis. Nuclei of aPSCs treated with VA-lip-siRNAHSP47 or with control agents were stained with FITC-TUNEL (green) and DAPI (blue) 72 h after each treatment. Arrowheads indicate apoptotic cells. Pictures taken at original magnification (×200) and magnified images

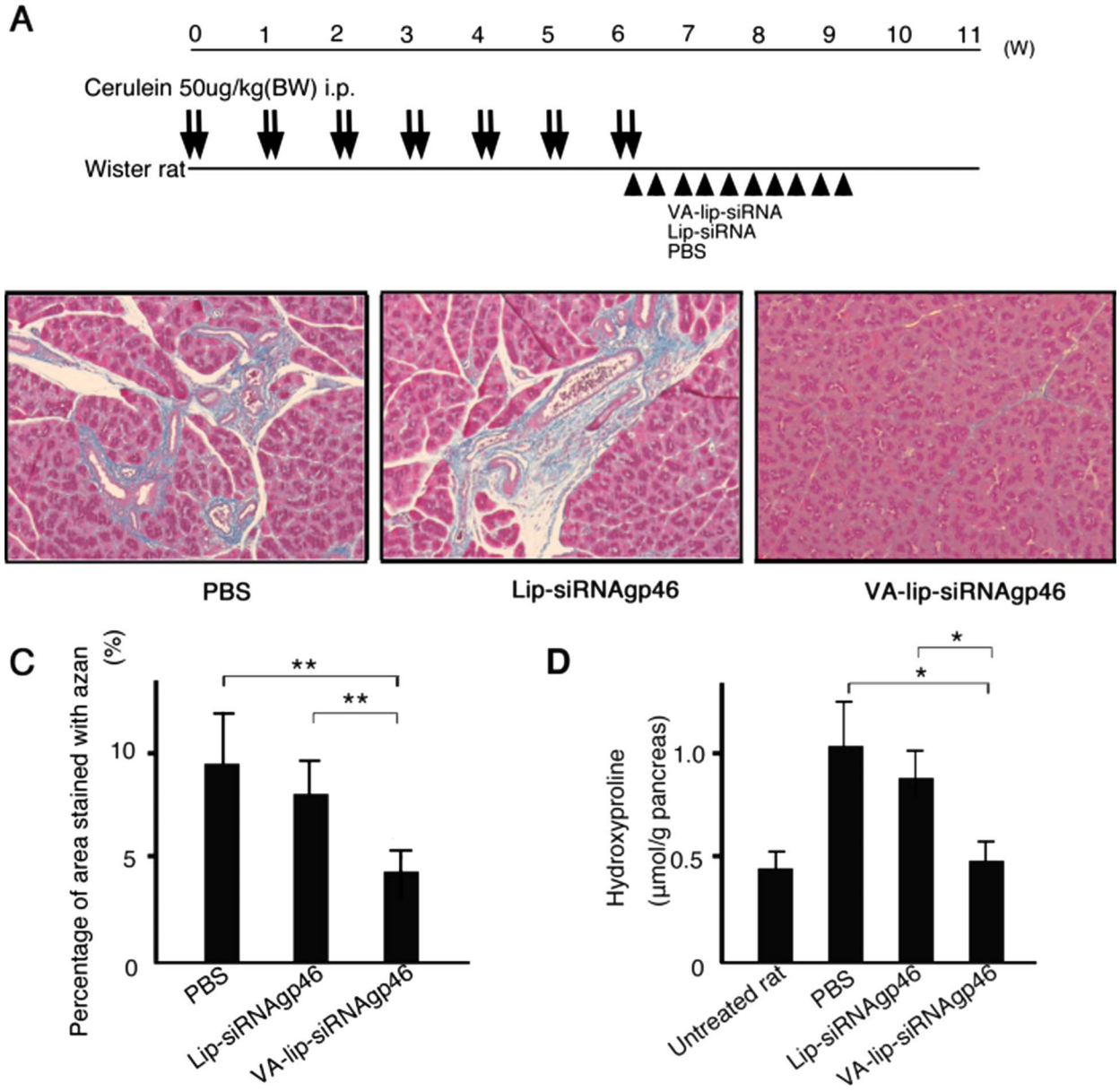

Figure 5 Effect of intravenous injected vitamin A-coupled liposomes (VA-lip-siRNAgp46) on cerulein-induced pancreatic fibrosis. (A) Schedule of VA-lip-siRNAgp46 treatment in rats with cerulean-induced pancreatic fibrosis. Samples were obtained from cerulean-treated rats that received 10 injections of VA-lip-siRNAgp46, Lip-siRNA gp46 (siRNA doses of 0.75 mg/kg, 3 times every other day) or PBS alone (n=10 per group). (B) Representative photomicrographs of an Azan-Mallory-stained pancreas section. Pictures taken at original magnification (×100). (C) Azan-Mallory-positive staining area assessed by computerised image analysis. Data were obtained from six randomly selected fields in each of 10 rats from three groups and represent the mean±SD. (D) Hydroxyproline content in the pancreas. Mean±SD of 10 rats per group. *p<0.05; **p<0.01 vs VA-lip-siRNAgp46 treated-dibutyltin dichloride rat.

Incidentally, regarding a possible role of other cellular components such as myofibroblasts in pancreatic fibrosis, it is rather difficult to distinguish it from that of aPSCs since when PSCs are activated, they become positive for α-SMA, which is characteristic of myofibroblasts. In this context, it should be noted that quiescent PSCs store vitamin A, and when they become

corresponding to the areas enclosed in boxes are presented in the inset. (D) Quantification of apoptotic aPSCs shown in figure 4C. Apoptotic nuclei (green) and total nuclei (green + blue) were examined by fluorescent microscopy and counted in 10 randomly selected fields per slide for each indicated treatment; the ratios of apoptotic to normal nuclei were expressed as percentages. Results represent the mean±SD of three independent experiments. *p<0.01 vs VA-lip-siRNAHSP47. (E) Representative immunohistochemical staining of pancreas specimens from dibutyltin dichloride (DBTC) (5 mg/kg) treated rats (day 56) that received six injections of VA-lip-siRNAgp46 (left panel) or VA-lip-siRNArandom (right panel) (siRNA doses of 0.75 mg/kg, 3 times every other day) stained for TUNEL (brown, arrowhead) and α-SMA (red). Magnified images of the corresponding areas in boxes indicated that the number of cells with TUNEL-positive overlapping of α-SMA-positive PSCs was substantially increased in VA-lip-siRNAgp46 specimens compared with VA-lip-siRNArandom specimens. Pictures were taken at original magnification (×100). (F) Quantification of TUNEL-positive PSCs in pancreas specimens from VA-lip-siRNAgp46-treated DBTC-rats and VA-lip-siRNArandom. The number of TUNEL-positive cells in α-SMA-positive areas was counted in 10 randomly selected fields per pancreas section of each rat. *p<0.01. The results were essentially similar within each group of three rats.

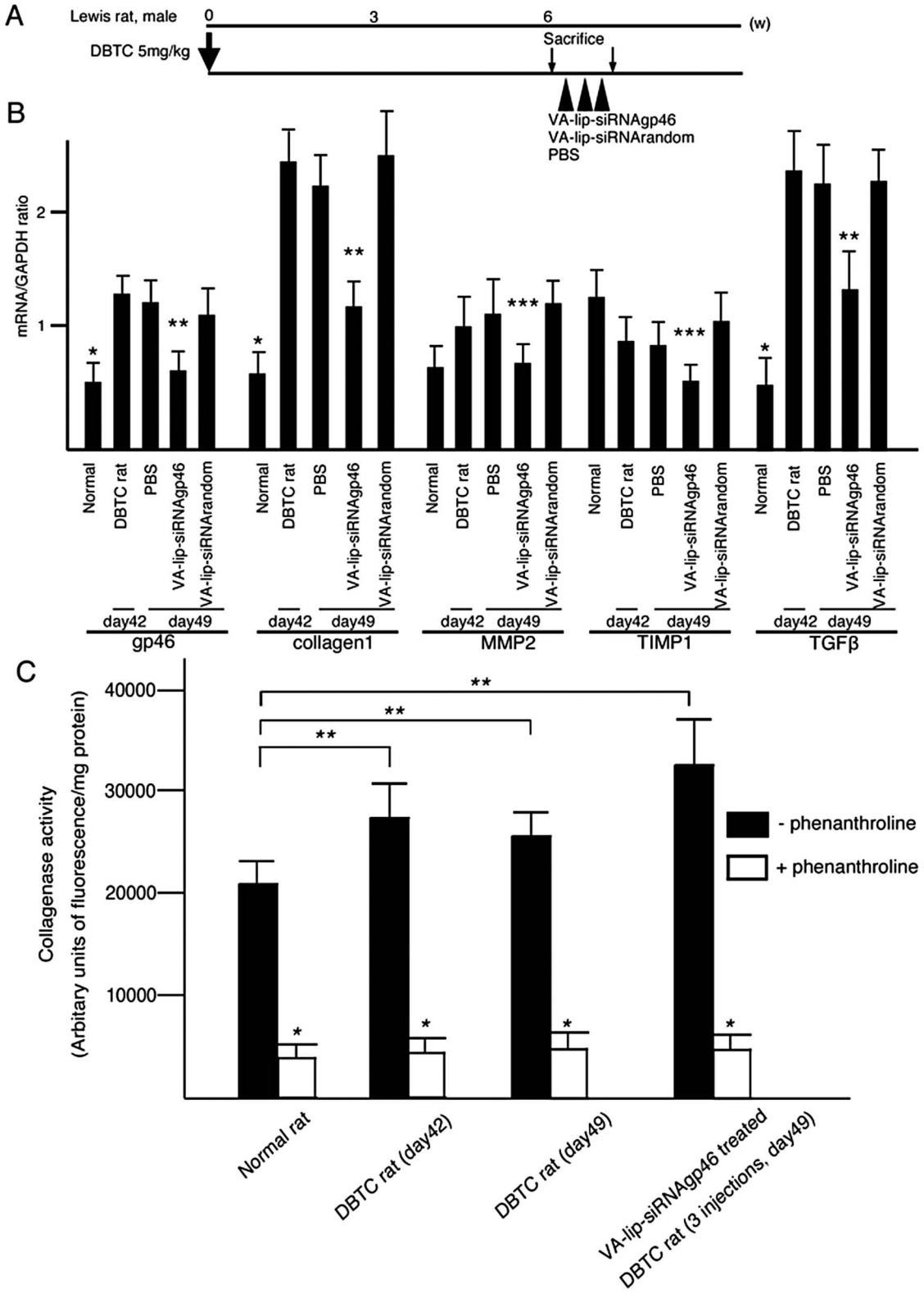

Figure 6 Effect of vitamin A-coupled liposomes (VA-lip-siRNAgp46) treatments on mRNA expression of fibrosis-related proteins and collagenase activity in pancreas homogenates. (A) Schedule of VA-lip-siRNAgp46 treatment in rats with dibutyltin dichloride (DBTC)-induced pancreatic fibrosis. Samples were obtained from DBTC-treated rats that received three injections of VA-lip-siRNAgp46, Lip-siRNA gp46 (siRNA doses of 0.75 mg/kg, 3 times every other day), or PBS alone (n=3 per group). (B) The expression of gp46, procollagen I, MMP-2, TIMP-1, and TGFβ mRNA in normal rats, DBTC-treated rats treated with three injections of PBS, DBTC-treated rats treated with three injections of VA-lip-siRNArandom, and DBTC-treated rats treated with three injections of VA-lip-siRNAgp46 were quantitated by real-time PCR. Expression was normalised as the ratio to GAPDH mRNA, a housekeeping gene. *p<0.01 vs DBTC rat (day42). **p<0.01 vs PBS (day46). ***p<0.05 vs PBS (day46). (C) Total collagenase activity in pancreas homogenates from normal rats, DBTC-treated rats (day 42), DBTC-treated rats (day 49), and DBTC rats treated with three injections of VA-lip-siRNAgp46 (siRNA doses of 0.75 mg/kg, 3 times every other day, day 49) in the absence or presence of MMP inhibitor (1,10-phenanthroline). Results are the mean±SD of five rats per group. *p<0.01 vs without inhibitor. **p<0.05 vs normal rat.

myofibroblasts, although no more vitamin A droplets in their cytoplasm are observed, they still can take up vitamin A as shown by in vitro transfection experiments using VA-lip-siRNAgp46. This was true for hepatic stellate cells too. This is carefully discussed in our previous paper.[6] It is speculated that deposited vitamin A in quiescent cells may be used up or partly excreted on myofibrobrast transformation.

Prior to the examination of therapeutic effect, we assured specific delivery of VA-lip-siRNAgp46 to aPSCs in fibrotic pancreas tissue, demonstrating the mergence of the green fluorescence of siRNA-FAM encapsulated in vitamin A liposomes with the red fluorescence of α-SMA-positive cells (aPSCs), and higher accumulation of ^{3}H-VA-lipsiRNA in the pancreas of DBTC-treated rats than that in normal rats. The reason for 10-fold more radioactivity in the lung and intestine may be due to the higher content of macrophages in these organs. However, the 150-fold difference between liver and pancreas may not be simply ascribed to the difference in macrophage content, but more likely to the increased number of activated hepatic stellate cells since in this model, not only pancreas but also liver undergoes fibrosis because of obstruction of the common bile duct.

Collectively these results supported the notion that aPSCs preferentially take up siRNAgp46 encapsulated in vitamin A liposomes in vivo. We also examined the kinetics of the effect in vivo, prior to assessment of therapeutic efficacy, and found that the suppression of gp46 expression lasted for 3 days after the injection of VA-lip-siRNAgp46. Thus, our therapy protocol involved injecting the drug three times per week.

The therapeutic effect of treatment, namely, histological improvement and normalised hydroxyproline levels in the pancreas, was observed following administration of drug 10 times. In our previous study using liver cirrhosis models, substantial resolution of fibrotic tissue was obtained after only five treatments.[6] In the present study, we also initially used only five treatments, but improvement of fibrosis was unsatisfactory. This may be due to the fact that the pancreas is relatively poor in blood supply compared with the liver, and thus the dosage of siRNAgp46 at the fibrotic loci supplied by five injections may not have been sufficient to bring about effective resolution of pancreatic fibrosis.

Incidentally, it may be noteworthy to mention that our treatment brought about less vessel density since it promises wider implications such as depletion of tumour stroma in pancreas cancer. In this regard, it is nowadays a well accepted concept that modality to normalise the vascularity by diminishing immature microvessels with anti-neoangiogenesis antibody, rather enhances the efficacy of chemotherapy when the antibody and anticancer drug are used in combination.[22]

Regarding the mechanism for the enhanced microvascularity in fibrotic tissue and decrement of vascularity after treatment, we assume, in good agreement with reports by and Hideshima and Okada,[23 24] that aPSCs are producing angiogenesis factor(s) which will be eradicated from the tissue in accordance with apoptosis induction by treatment. This assumption is based on our recent finding that rat aPSCs are indeed expressing some angiogenesis factors, including fibroblast growth factor (unpublished observation).

The resolution of fibrosis appears to occur by a dual mechanism involving siRNAgp46, which inhibits de novo secretion of collagen, and tissue collagenase, which dissolves predeposited collagen matrix. This assumption is consistent with the fact that collagenase activity in the pancreas at day 42 and day 49 after DBTC treatment, when massive fibrosis occurred, was higher than that of normal pancreas. The reason for sustained high collagenase activity after VA-lip-siRNAgp46 treatment, despite the suppressed MMP2 mRNA, may be that TIMP from aPSCs is also reduced due to apoptosis of aPSCs. In addition, a persistent extracellular matrix pool of collagenase after it is secreted from cells may account for the sustained collagenase activity.[25 26] Activation of matrix metalloproteinases (MMPs) derived from inflammatory cells by reduced TIMP-1 expression may also account for the discrepancy.

Furthermore, apoptosis of aPSCs via transduction of siRNAgp46 was confirmed in our vitro experiment, indicating that a similar mechanism is involved in apoptosis of aHSCs and aPSCs. It is plausible that collagen secreted by aHSCs and aPSCs serves as a survival signal and that this signal is abrogated, leading to apoptosis, as a result of collagen degradation by collagenase (unpublished observation). In support of this possibility, our results demonstrated that high collagenase activity was maintained in the pancreas even after treatment (figure 6C). Incidentally, induction of apoptosis by inhibiting collagen secretion was confirmed to occur even in human PSCs treated with VA-lip-siRNAHSP47, indicating applicability of this approach in the clinical setting.

Interestingly, inflammation associated with fibrosis in this model was also decreased by this treatment, probably due to the fact that aPSCs, which were eradicated by our treatment, are involved not only in the development of fibrosis but also in the inflammatory reaction.[21]

Liver fibrosis in DBTC-treated rats was also successfully resolved with treatment in the present study. However, because the epithelial plug in the common duct was not removed by the treatment, increased serum amylase, alanine aminotransferase and bilirubin persisted (data not shown). In the DBTC model, unlike in advanced chronic pancreatitis in humans, β-cells remained intact and, therefore, no change in blood glucose levels was observed throughout the experimental period (data not shown).

To further evaluate the therapeutic effect of our modality in another model, we established a chronic pancreatitis model based on repeated administration of cerulein to rats.[12 18] The results in this model were compatible with those of the DBTC model, confirming the general efficacy of our modality in dissimilar pancreatic fibrosis models.

Off-target effects and stimulation of toll-like receptors (TLRs) are both critical issues to be solved in the application of therapies using siRNA. Since we used the same siRNA as that of the previous study on liver cirrhosis in which we denied a bystander effect by demonstrating comparable gene silencing efficacy and antifibrotic effect with two other independent siRNAs against the same target,[6] we believe it is unlikely to be the case.

Nonetheless, for future clinical applications, it will be necessary to conduct careful explorations of adverse effects, off-target effects and TLR stimulation.

In conclusion, the present data clearly indicate the therapeutic potential of our modality for pancreas fibrosis and suggest its potential for the treatment of organ fibrosis.

Contributors HI, YS and KM designed research, performed experiments and wrote the paper. AY, RF, HN, NB, TH, TS, KM, RT, MK, SA, YK, KH and JK performed experiments. YN designed research, wrote the paper and supervised the whole project. All authors discussed the results and commented on the manuscript.

Competing interests None.

Provenance and peer review Not commissioned; externally peer reviewed.

REFERENCES

1 Bachem MG, Schneider E, Gross H, *et al*. Identification, culture, and characterization of pancreatic stellate cells in rats and humans. *Gastroenterology* 1998;115:421–32.
2 Schneider E, Schmid-Kotsas A, Zhao J, *et al*. Identification of mediators stimulating proliferation and matrix synthesis of rat pancreatic stellate cells. *Am J Physiol Cell Physiol* 2001;281:C532–43.

3 Shimizu K, Shiratori K, Kobayashi M, *et al*. Troglitazone inhibits the progression of chronic pancreatitis and the profibrogenic activity of pancreatic stellate cells via a PPARgamma-independent mechanism. *Pancreas* 2004;29:67–74.
4 Yamada T, Kuno A, Masuda K, *et al*. Candesartan, an angiotensin II receptor antagonist, suppresses pancreatic inflammation and fibrosis in rats. *J Pharmacol Exp Ther* 2003;307:17–23.
5 Kuno A, Yamada T, Masuda K, *et al*. Angiotensin-converting enzyme inhibitor attenuates pancreatic inflammation and fibrosis in male Wistar Bonn/Kobori rats. *Gastroenterology* 2003;124:1010–19.
6 Sato Y, Murase K, Kato J, *et al*. Resolution of liver cirrhosis using vitamin A-coupled liposomes to deliver siRNA against a collagen-specific chaperone. *Nat Biotechnol* 2008;26:431–42.
7 Buchholz M, Kestler HA, Holzmann K, *et al*. Transcriptome analysis of human hepatic and pancreatic stellate cells: organ-specific variations of a common transcriptional phenotype. *J Mol Med* 2005;83:795–805.
8 Apte MV, Haber PS, Applegate TL, *et al*. Periacinar stellate shaped cells in rat pancreas: identification, isolation, and culture. *Gut* 1998;43:128–33.
9 Williams EJ, Benyon RC, Trim N, *et al*. Relaxin inhibits effective collagen deposition by cultured hepatic stellate cells and decreases rat liver fibrosis in vivo. *Gut* 2001;49:577–83.
10 Inoue M, Ino Y, Gibo J, *et al*. The role of monocyte chemoattractant protein-1 in experimental chronic pancreatitis model induced by dibutyltin dichloride in rats. *Pancreas* 2002;25:e64–70.
11 Merkord J, Jonas L, Weber H, *et al*. Acute interstitial pancreatitis in rats induced by dibutyltin dichloride (DBTC): pathogenesis and natural course of lesions. *Pancreas* 1997;15:392–401.
12 Elsasser HP, Haake T, Grimmig M, *et al*. Repetitive cerulein-induced pancreatitis and pancreatic fibrosis in the rat. *Pancreas* 1992;7:385–90.
13 Puig-Divi V, Molero X, Salas A, *et al*. Induction of chronic pancreatic disease by trinitrobenzene sulfonic acid infusion into rat pancreatic ducts. *Pancreas* 1996;13:417–24.
14 Merkord J, Weber H, Jonas L, *et al*. Influence of ethanol on long-term effects of dibutyltin dichloride (DBTC) in pancreas and liver of rats. *Hum Exp Toxicol* 1998;17:144–50.
15 Yamamoto M, Otani M, Otsuki M. A new model of chronic pancreatitis in rats. *Am J Physiol Gastrointest Liver Physiol* 2006;291:G700–8.
16 Tsuchitani M, Saegusa T, Narama I, *et al*. A new diabetic strain of rat (WBN/Kob). *LabAnim* 1985;19:200–7.
17 Sparmann G, Merkord J, Jaschke A, *et al*. Pancreatic fibrosis in experimental pancreatitis induced by dibutyltin dichloride. *Gastroenterology* 1997;112:1664–72.
18 Ishibashi T, Zhao H, Kawabe K, *et al*. Blocking of monocyte chemoattractant protein-1 (MCP-1) activity attenuates the severity of acute pancreatitis in rats. *J Gastroenterol* 2008;43:79–85.
19 Iredale JP, Benyon RC, Pickering J, *et al*. Mechanisms of spontaneous resolution of rat liver fibrosis. Hepatic stellate cell apoptosis and reduced hepatic expression of metalloproteinase inhibitors. *J Clin Invest* 1998;102:538–49.
20 Weidenbach H, Lerch MM, Turi S, *et al*. Failure of a prolyl 4-hydroxylase inhibitor to alter extracellular matrix deposition during experimental pancreatitis. *Digestion* 1997;58:50–7.
21 Masamune A, Watanabe T, Kikuta K, *et al*. Roles of pancreatic stellate cells in pancreatic inflammation and fibrosis. *Clin Gastroenterol Hepatol* 2009;7: S48–54.
22 Jain RK. Normalizing tumor vasculature with anti-angiogenic therapy: a new paradigm for combination therapy. *Nat Med* 2001;7:987–9.
23 Hideshima K, Seike J, Mimura S, *et al*. HSP47 and angiogenic factor expression and its implication for the healing of periosteal defects in the mouse cranium. *Oral Med Pathol* 2006;11:27–33.
24 Okada H, Inoue T, Kanno Y, *et al*. Selective depletion of fibroblasts preserves morphology and the functional integrity of peritoneum in transgenic mice with peritoneal fibrosing syndrome. *Kidney Int* 2003;64:1722–32.
25 Zhou X, Hovell CJ, Pawley S, *et al*. Expression of matrix metalloproteinase-2 and -14 persists during early resolution of experimental liver fibrosis and might contribute to fibrolysis. *Liver Int* 2004;24:492–501.
26 Steffensen B, Wallon UM, Overall CM. Extracellular matrix binding properties of recombinant fibronectin type II-like modules of human 72-kDa gelatinase/type IV collagenase. High affinity binding to native type I collagen but not native type IV collagen. *J Biol Chem* 1995;270:11555–66.

Supplementary figure 1. Induction of pancreatic fibrosis by DBTC treatment

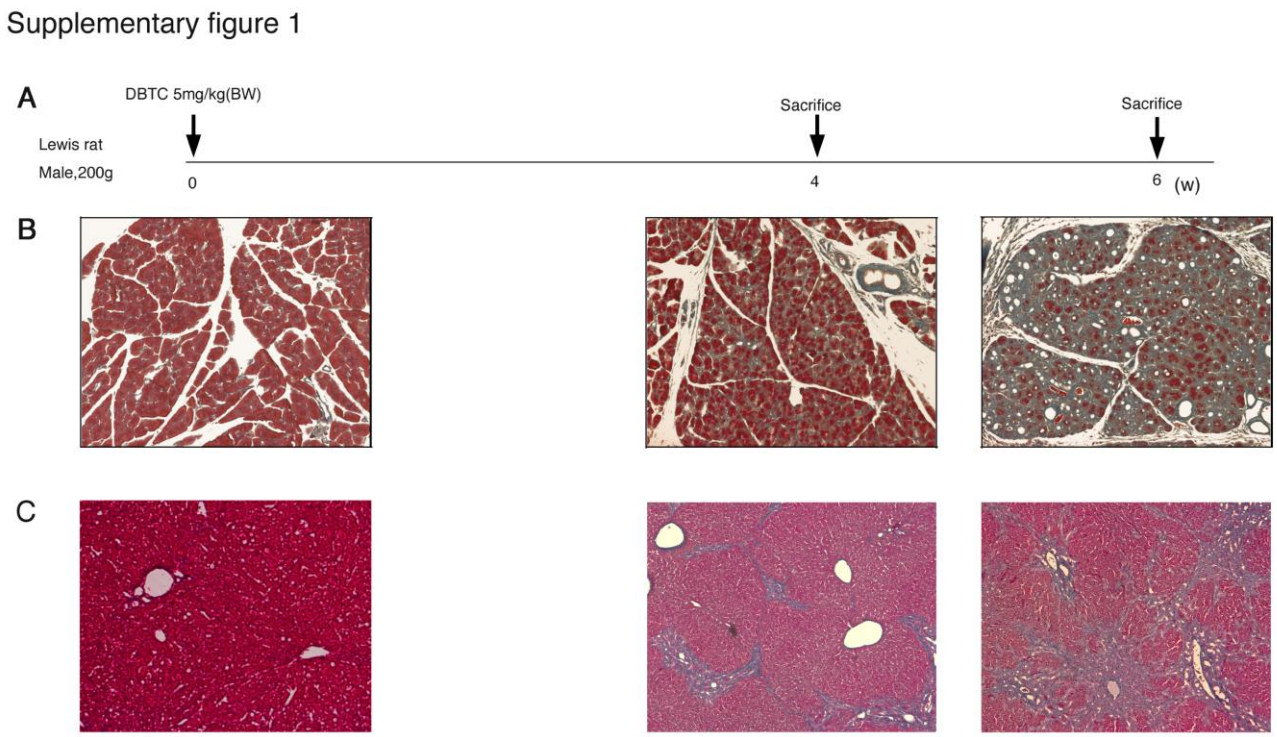

(***A***) Schedule of induction of pancreatic fibrosis by DBTC. DBTC (5 mg/kg body weight) was injected into the right jugular vein. At days 29, 43 after application of DBTC, rats were killed and the pancreases were obtained. ***(B)*** Representative photomicrographs of Azan-Mallory-stained pancreas section**s** at day 0, 29 and 43 after administration of DBTC. Pictures taken at original magnification (x 100). At day 29, early deposition of connective tissue was observed with a predominance in periductal areas. At day 43, the pancreatic tissue was characterized by extended interstitial and periductal fibrosis, cellular infiltrates, and tubular complexes. ***(C)*** Representative photomicrographs of Azan-Mallory-stained liver sections at day 0, 29, and 43 after administration of DBTC. Pictures were taken at original magnification (x 100).

Supplementary figure 2. Induction of pancreatic fibrosis by cerulein treatment

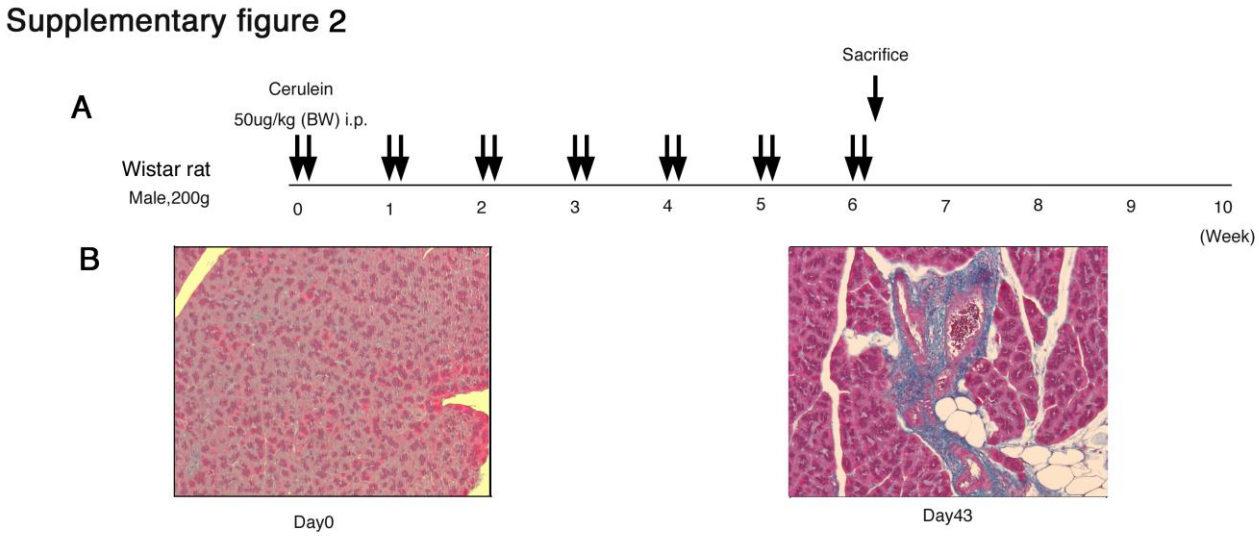

(A) Schedule of induction of pancreatic fibrosis by cerulein. Cerulein (50 μg/kg body weight) were induced in rats by 2 intraperitoneal injections of cerulein (50 μg/kg) given 1 hour apart. At day 43 after the first application of cerulein, rats were killed and the pancreases were removed. ***(B)*** Representative photomicrographs of Azan-Mallory–stained pancreas section at day 0 and 43 after application of DBTC. Pictures taken at original magnification (x 100). At day 43, deposition of connective tissue was observed with a predominance of periductal areas.

Supplementary figure 3. Duration of suppressive effect of siRNAgp46 on gp46 expression in aPSCs

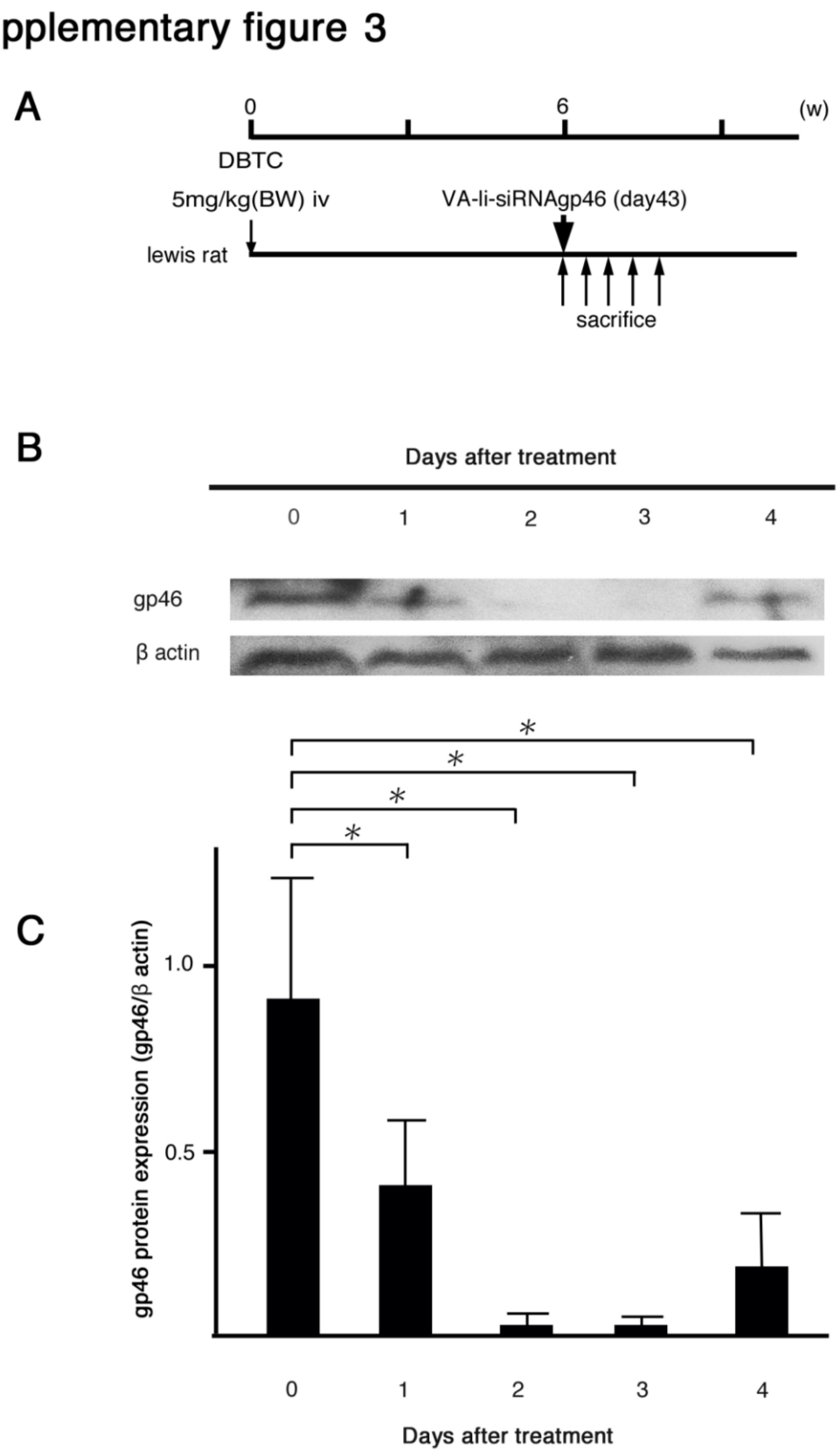

(A) The time course of gp46 expression in a rat with DBTC-induced pancreatic fibrosis treated with VA-lip-siRNAgp46 (siRNA 0.75 mg/kg, one injection at day 43, n=15). Western blotting ***(B)*** and quantitative densitometry analysis ***(C)*** were carried out to measure the expression of gp46 at the time points indicated. The expression of gp46 was normalized to that of β-actin. *$p < 0.05$ vs day 0.

Supplementary figure 4. Effect of VA-lip-siRNAgp46 treatment on pancreatic inflammation of DBTC-treated rats

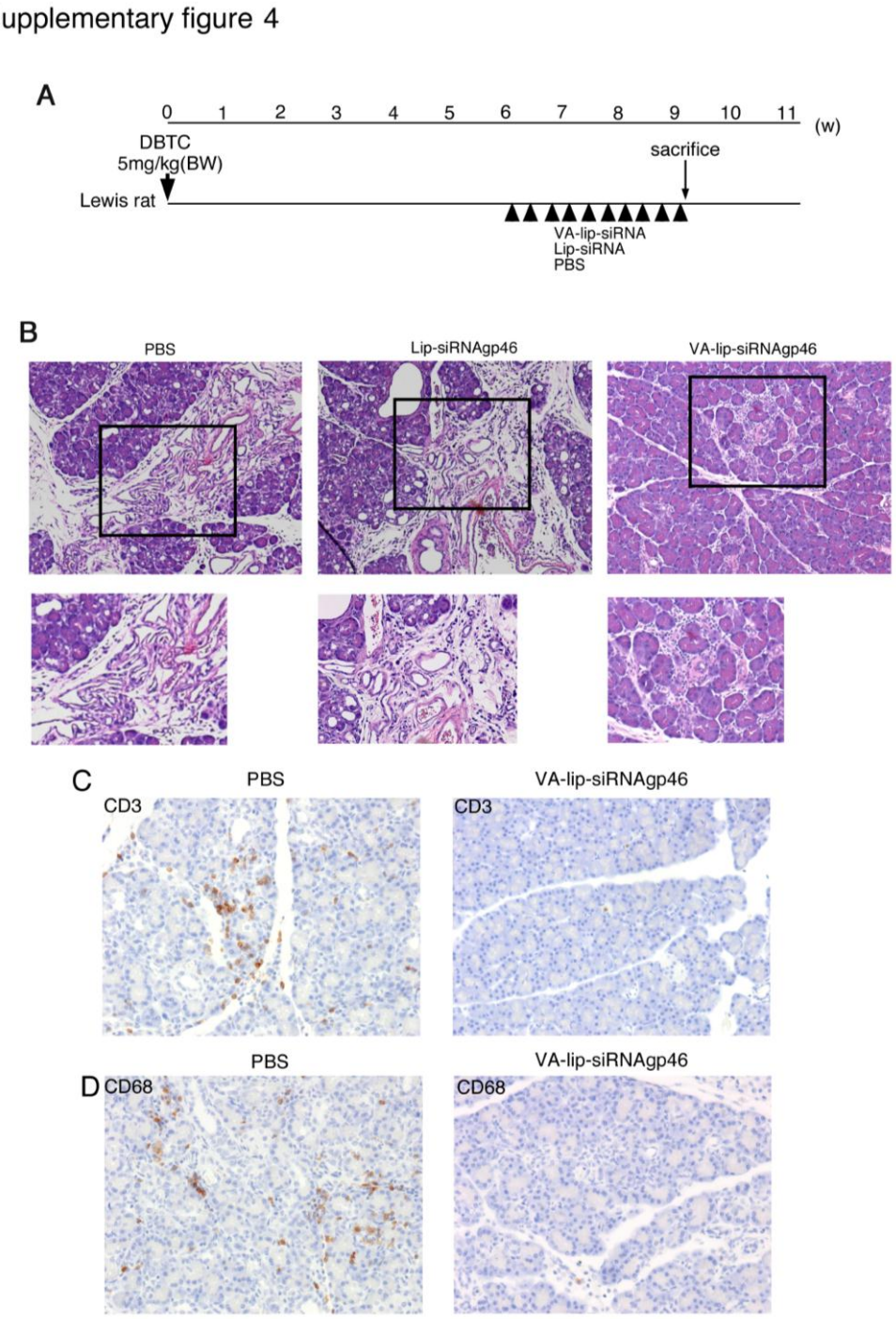

(A) Schedule of VA-lip-siRNAgp46 treatment in rats with DBTC-induced pancreatic fibrosis. Samples were obtained from DBTC-treated rats that received 10 injections of VA-lip-siRNAgp46 (siRNA doses of 0.75 mg/kg, 3 times every other day), Lip-siRNAgp46 or PBS alone (n= 10 per group).
(*B*) Representative photomicrographs of pancreas section. Representative photomicrographs of Hematoxylin-eosin stained pancreas section (original magnification x 100). Magnified images (x200) corresponding to the areas enclosed in boxes are presented as indicated. ***(C)*** Representative immunohistochemical staining images of T cells stained with anti CD3 antibody (original magnification x 50). ***(D)*** Representative immunohistochemical staining images of macrophages stained with anti CD68 antibody (original magnification x 200). Results from each group of 10 rats were essentially similar (B-D).

Supplementary figure 5. Effect of i.v. injected VA-lip-siRNAgp46 on DBTC-induced hepatic fibrosis

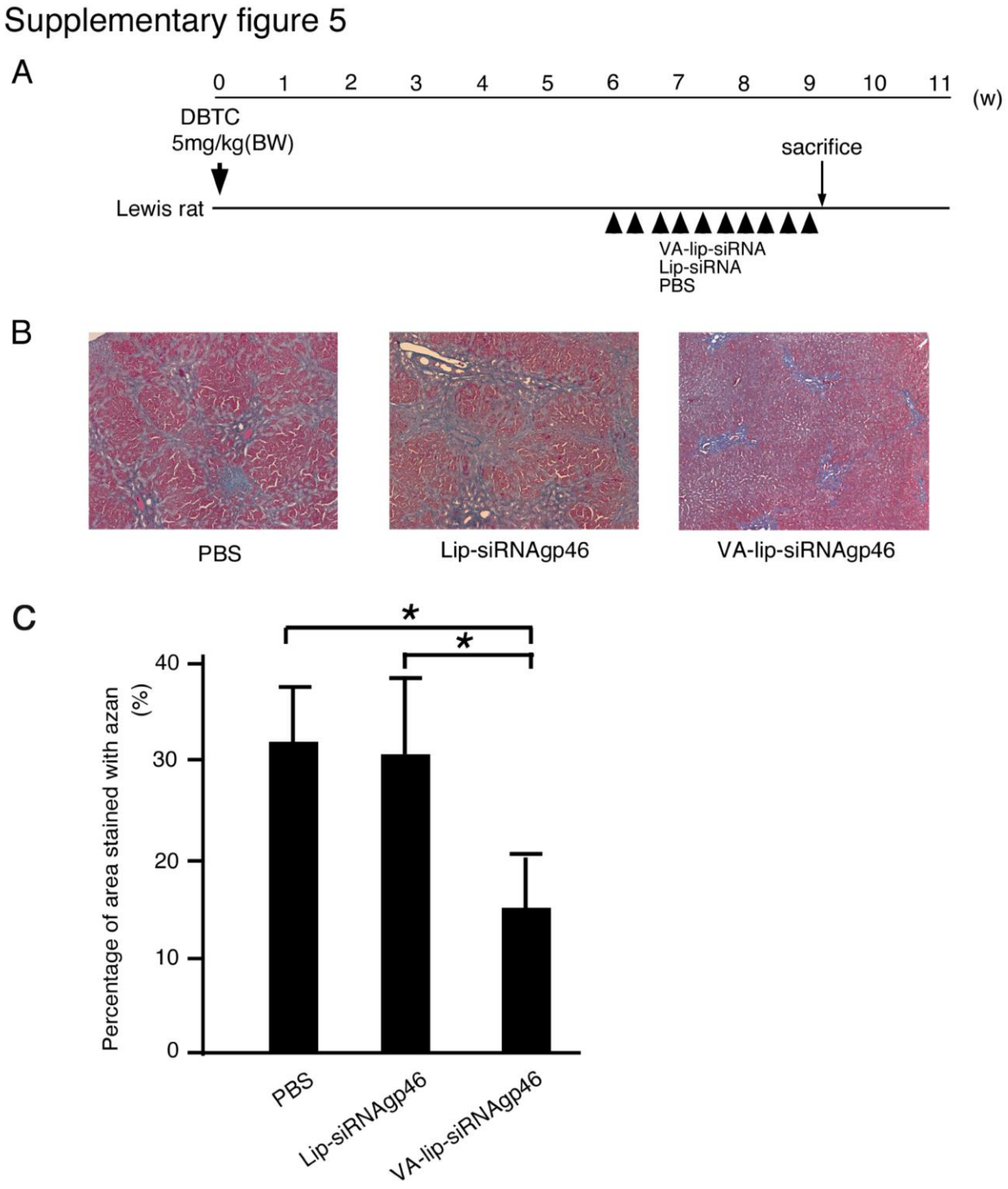

(A) Schedule of VA-lip-siRNAgp46 treatment in rats with DBTC-induced hepatic fibrosis. Samples were obtained from DBTC-treated rats that received 10 injections of VA-lip-siRNAgp46, Lip-siRNA gp46 (siRNA doses of 0.75 mg/kg, 3 times every other day), or PBS alone (n = 10 per group). ***(B)*** Representative photomicrographs of Azan-Mallory-stained pancreas sections (original magnification x 100). ***(C)*** Azan-Mallory–positive staining area assessed by computerized image analysis. Data were obtained from 6 randomly selected fields in each of 10 rats from 3 groups and represent the mean ± SD. *$p < 0.05$ vs VA-lip-siRNAgp46 treated- DBTC rat.

Supplementary figure 6. Microvessel density before and after administration of VA-lip-siRNAgp46 treatment on pancreas of DBTC-treated rats

Supplementary figure 6

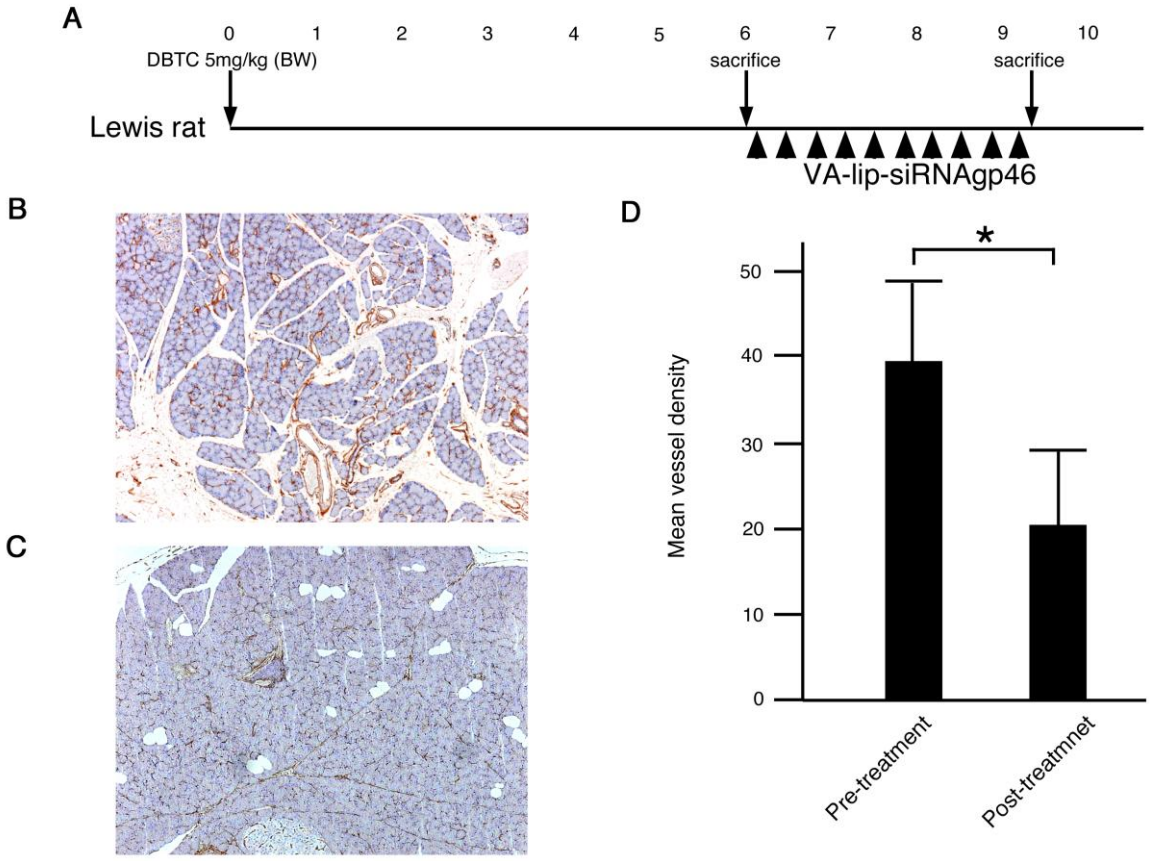

(A) Schedule of VA-lip-siRNAgp46 treatment in rats with DBTC-induced pancreatic fibrosis. Samples were obtained from DBTC-treated rats on day 42 before treatment of VA-lip-siRNAgp46 and from DBTC-treated rats that received 10 injections of VA-lip-siRNAgp46 on day 65 (siRNA doses of 0.75 mg/kg, 3 times every other day (n= 10 per group). ***(B)*** Representative immunohistochemical staining images of vessels stained with anti CD34 antibody on day 42. Pictures were taken at original magnification (x 50). ***(C)*** Representative immunohistochemical staining images of vessels stained with anti CD34 antibody on day 65. Pictures were taken at original magnification (x 50). ***(D)*** MVD was analyzed as described in the Materials and Methods. Mean ± SD of 10 rats per group. *$p < 0.05$

Supplementary table 1

Inflammatory parameters in the DBTC pancreas treated with VA-lip-siRNAgp46 or Lip-siRNAgp46 or PBS

	DBTC rat (Day 43)	PBS (Day 65)	Lip-siRNAgp46 (Day 65)	VA-lip-siRNAgp46 (Day 65)	P value of comparison between VA-lip-siRNA and other groups
Inflammatory cell infiltration	2.9 ± 0.6	2.6 ± 0.5	2.3 ± 0.5	0.8 ± 0.3	< 0.01
Fatty change	1.8 ± 0.5	1.5 ± 0.3	1.5 ± 0.4	0.5 ± 0.2	< 0.01
Tubular complex	2.1 ± 0.8	2.0 ± 0.8	1.8 ± 0.5	0.9 ± 0.2	< 0.01

Values are means ± SD (n=10)

Note. The grade of inflammation was defined according to a system reported previously (Takano S, et al. Effects of stress on the development of chronic pancreatitis. Pancreas 1992;7:548-555). Histological findings of chronic pancreatitis such as inflammatory cell infiltration,tubular complexes, and fatty changes were calculated as the sum of the lesion size scores per rat. Lesion size scores were as follows:
0 = absent; 1 = lesion appearing slightly in the lobule or intralobular region ; 3 = lesion evident across the lobule and intralobule region or showing destruction of lobular architecture. Value are means ± SD (n=10).

Supplementary methods

Immunohistochemical staining for macrophages and T cells.
Immunohistochemical staining for CD68 (macrophages) and CD3 (T cells) was performed by the dextran polymer method using monoclonal anti CD68 antibody (1: 100, DAKO), monoclonal anti CD3 antibody (1: 100, Nichirei Biosciences, Tokyo, Japan) and an Envision Kit (Dako), followed by color development with DAB and nuclear staining with Gill's hematoxylin solution. The grade of inflammation was defined according to a criteria reported previously.[1] Histological findings of chronic pancreatitis such as inflammatory cell infiltration, tubular complexes, and fatty changes were calculated as the sum of the lesion size scores per rat. Lesion size scores were as follows: 0 = absent; 1 = lesion appearing slightly in the lobule or intralobular region; 3 = lesion evident across the lobule and intralobule region or showing destruction of lobular architecture.

Measurement of microvascular density (MVD)
For evaluation of MVD, sections of pancreas tissue from the DBTC treated rat were stained with polyclonal anti CD34 antibody (1: 50, R&D Systems, Minneapolis, MN) as described in previous section, 8 fields of the stained section randomly selected were numerized at a magnification of ×200 through microscopy. The number of CD34 positive structures in each numerized image was then counted. The mean MVD for each section was calculated as the mean of the counts, after exclusion of the lowest and highest values measured.[2]

Supplementary reference

1. Takano S, Kimura T, Yamaguchi H, et al. Effects of stress on the development of chronic pancreatitis. Pancreas 1992;7:548-555.

2. Weidner N, Semple JP, Welch WR, et al. Tumor angiogenesis and metastasis--correlation in invasive breast carcinoma. N Eng J Med 1991;324:1-8.